



Performance of Lateral Torsional Buckling in Simple Steel T-beams with Openings

Ahmed AwadAllah*, Nasser Z. Ahmed¹

*Teaching Assistant, Department of Civil Engineering, Beni-Suef University, Egypt.

¹Associate Professor, Department of Civil Engineering, Beni-Suef University, Egypt

ARTICLE INFO

Article history:

Received: 10-02-24

Accepted: 01-05-24

Online: 27-05-24

Keywords: Lateral Torsional Buckling; T-Section; Finite Element; Openings.

ABSTRACT

T-shaped beams are very vulnerable to failure from lateral torsional buckling when they are bent. On the other hand, not much previous study has been done on the lateral torsional buckling behavior of T-shaped beams, especially those that have stem holes in them. This work aims to analyze the behavior of T-shaped beams with apertures under concentrated loads mid-span and evenly distributed loads using numerical methods. Furthermore, the objective of this research is to assess the impact of the moment gradient component, opening size, flange thickness, and stem thickness. A finite element program was used to create 3D finite element models for 108 T-beams in order to achieve this goal. This analysis takes material nonlinearity and beam geometric defects into account. A thorough parametric analysis was then carried out to investigate the many elements influencing the moment gradient factor of the T-beams that were being considered. The findings show that the factors under investigation have a major effect on how T-shaped beams behave. Moreover, it was found that the instantaneous magnification factor used in the lateral torsional buckling computation is adversely impacted by the existence of apertures.

1. Introduction

T-shaped beams are typically distinct from I-sections but can serve in load applications akin to them. On the other hand, T-sections are far more susceptible to an issues known as lateral-torsional buckling (LTB), in which the beam's compression flange twists and goes both laterally and vertically. Investigations on (LTB) in T-shaped beams, especially those with openings, have been limited for decades, despite numerous studies on LTB in a variety of beam types, such as double and single symmetric I-shaped

beams [1-4]. There are closed-form techniques to calculate the critical moment of LTB in I-section beams under consistent moment loading; however, in order to handle different load conditions, a moment gradient component should be added.

Studies on the assessment of the moment gradient factor of T-shaped beams are limited. It is important to note that [5,6] conducted the only studies in this area. A simple beam with moment gradients at both ends was examined in [5] using an energy-based method. The suitability of T-shaped beams' moment gradient factor in both the elastic and inelastic stages was examined by [6]. In their investigation, they also took residual stress and geometric imperfection into account, and they compared their findings with those obtained using various design codes. It was concluded that the LTB moment is not greatly impacted by introducing residual stress.

*Ahmed AwadAllah, Teaching Assistant-Faculty of Engineering-Beni-Suef University, Beni-Suef, mobile no. 01202542015, and ahmed.awadallah@eng.bsu.edu.eg.

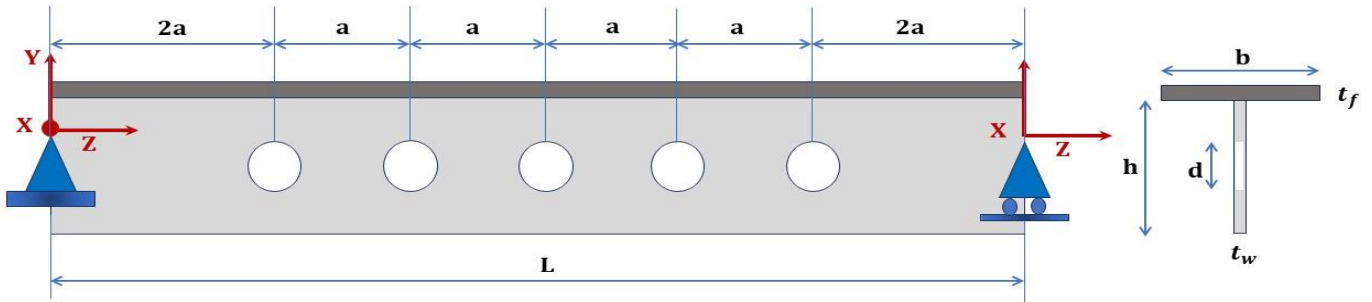


Fig. 1. The problem's geometry under study

[7] provided a precise formula that takes into account the connection between LTB and the failure modes of the beams, such as distortional and local buckling, to determine the buckling load of thin-walled beams. Accurate representation was given to complex phenomena, such as the load height effect resulting from the interplay between the cross-section rotation and the wall's relative rotation. An in-depth analytical analysis of the lateral-torsional buckling of simply supported beams with evenly distributed load and moment-affected apertures was provided in [8]. They used the total potential energy principle to construct an analytical equation for the LTB moment. The analytical model was validated using a three-dimensional model. The study concluded that, rather than merely averaging the critical moments or loads determined from the full and reduced section properties, the critical moment should be computed using the average torsional constant of the full and reduced sections.

Several studies have investigated the strength of steel beams with web openings and proposed methodologies for their design [9-12]. These researchers utilized a three-dimensional model to validate their analytical approach. Their findings concluded that instead of merely averaging the critical moments or loads calculated from the full and reduced section properties, it is more accurate to calculate the critical moment based on the average torsional constant of both sections.

To evaluate the LTB behavior of steel beams having web holes, extensive numerical simulations were conducted [13–17]. [18] studied the behavior of steel beams with circular web apertures using the finite element approach. They created a three-dimensional model that takes into account the beam's potential failure modes and carried out a thorough parametric analysis to assess the impact of different geometrical parameters on the stability of the beam. All potential modes of failure and their corresponding moment gradient factors were reported.

[19] used numerical analysis to examine the impact of cellular web perforations on the elastic lateral stability of steel beams. A thorough parametric analysis showed that the moment gradient factor is highly dependent on the beam geometry and slenderness. The study also demonstrated that web distortion rises with decreasing beam slenderness, resulting in a lateral distortional buckling mode linked to a moment gradient factor that is lower than that advised by design rules for solid beams.

In their study, [20] utilized nonlinear numerical modeling to analyze the failure loads and load-deflection behavior of both normal and high-strength cellular steel beams. Additionally, a parametric investigation was performed on 120 cellular beams to assess how changes in beam geometry, span, and material properties influence their lateral-torsional buckling (LTB). Throughout the investigation, a midspan-focused load was employed. The combined effect of web distortion and web-post buckling was found to significantly reduce the load-carrying capacity of the beams. He also demonstrated how cellular steel beams with low slenderness may support a significantly greater load when they are made of high-strength steel.

There aren't many finite element analyses or experimental test findings on T-shaped beams, especially those with stem holes, according to the literature survey above. The aim of this work is to

- investigate LTB to determine the moment gradient factor of the beam with holes.
- Examine how the web thickness, flange thickness, and aperture size affect the T-shaped beams' inelastic LTB.

This paper presents a comprehensive study on T-shaped beams, incorporating various geometric dimensions of stem openings. A detailed 3D finite element model was developed using ABAQUS software [21]. The validity of the model parameters was confirmed through comparisons with theoretical, numerical, and experimental data from existing literature. Subsequently, the validated model was utilized to

perform an extensive parametric study, comprising the establishment of 81 distinct models to fulfill the objectives of the research.

2. Problem Outline

The study takes into account the geometry of a T-shaped beam, which is identified by its span (L), stem height (h), stem thickness (t_w), and flange width (b), flange thickness (t_f). Along the span, there are round apertures with a diameter that are uniformly spaced apart. The beam includes many standard panels of width S , each with a single opening, corresponding to an even integer-valued length-to-opening spacing ratio L/a . The geometry of a common T-shaped beam with stem holes is depicted in Figure 1. With a roller at its right end and a hinge at its left, a simply supported beam is used. The T-shaped section's center of gravity is where the supports are situated.

Moreover, a cartesian coordinate system is employed, with the Z -axis running down the beam length and the Y -axis down with the beam depth. By placing stiffener plates at the ends of the beam, intense reaction-related localized web yielding is prevented. To classify the commonly used practical dimensions of T-shaped beams with apertures, a thorough survey has been conducted. The current work considers a total of 54 different geometrical configurations; however, as each configuration is examined under two distinct load situations, 108 finite element analyses are given.

The dimensions of the Tee section are selected to cover the three section categories—compact, non-compact, and slender—as defined by the Egyptian code. Table 1 summarizes the range of dimensions that were used. For flange width (b) and stem depth (h), a single value is assigned to each of the examined beams.

Table 1
Numerical characteristics

L (mm)	t_w (mm)	t_f (mm)	d/h
5400	10	12	0.5
6300	8	6	0.6
7200	6	-	0.8

3. Numerical Model

ABAQUS, a general-purpose finite element program, was used to create the numerical finite element model in this investigation [29]. One significant method that is frequently used to forecast buckling loads is the Riks method provided by ABAQUS. The process includes boundary conditions and nonlinear materials. Applying general-purpose numerical

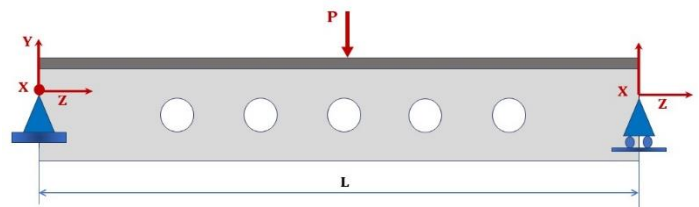
analysis, determine the critical moment of T-shaped beams with openings.

The initial step in the analysis process is to perform linear buckling analysis, where the results of the stage are the buckling forms and buckling loads. Considering the findings of the first stage, inelastic buckling analysis is next carried out using the arc-length approach or Riks analysis. The general-purpose S4 shell element is used to model the Tee-shaped beams (with full integration). This element is perfect for a study involving massive rotations and finite membrane strains because it has four corner nodes with six degrees of freedom. To get accurate results, the flange and the stem of the Tee beam have meshed such that there are six elements per flange width and 16 elements per web height.

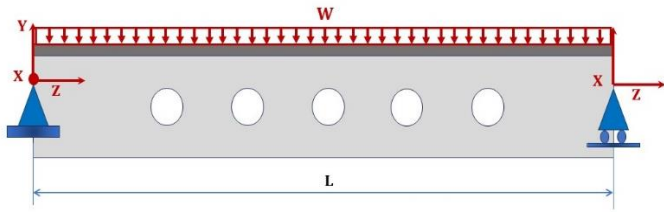
With a Poisson's ratio of $\nu = 0.3$ and a Young's modulus of $E = 210$ GPa, the T-shaped beam is thought to have linear elastic material for elastic analysis. Since it has multi-linear isotropic and kinematic hardening, the beam material for nonlinear analysis is thought to be elastoplastic. The constituents of this multi-linear material model are the yield stress F_y , ultimate stress F_u , Poisson's ratio ν , initial elastic Young's modulus E , strain hardening modulus E_t , among others. The study used carbon steel from Salmon et al. [18] with the following parameters: unless otherwise noted, $E = 210$ GPa, $E_t = 6.3$ GPa, $\nu = 0.3$, $F_y = 250$ MPa, $F_u = 400$ MPa, and $\epsilon_2 = 0.014$ correspond to the typical properties of the steel.

Figure 1 illustrates the boundary conditions. The left support restricts vertical (U_y), lateral (U_x), and longitudinal (U_z) displacements, while the right support confines both vertical and lateral displacements. Additionally, torsional rotation is prevented throughout the beam's length.

The two distinct load categories that have been taken into consideration in this study are shown in Figure 2. They consist of equal and opposite end moments, a homogeneous distributed load, and a concentrated mid-span load. At the shear center of the T-shaped beam, a concentrated and uniform load is given to prevent stabilizing and destabilizing effects. To prevent web crippling, the focused load is applied to a square region.



(a) Mid-span concentrated load



(b) Uniform distributed load

Fig.2. Types of applied load a. mid-span concentrated load b. uniform distributed load

Many research have been performed on I-shaped beams either with or without web holes, however very few or none were found about T-shaped beams with or without slots. Hence, theoretical, numerical, and experimental models of T-shaped sections without openings and I-shaped sections with and without web openings from the literature were utilized to confirm the material models, element types, mesh size, and analytical technique used in this study. The numerical model was constructed having the same shape and material attributes that were specified in the selected literature that was utilized for validation.

4. Modal Validation

Simply supported T-beams' elastic lateral buckling under moment gradient was studied by (Kitipornchai and Wang 1985). A study was conducted to ascertain the critical moment under a uniform moment of T-beams with different lengths (3, 6, 9, and 12 meters). As a result, the accuracy of the finite element model represented by the elastic buckling capacity in this research is verified by means of these beams' results. A free program called LTB beam, which is intended for the research of lateral-torsional buckling, is also used to evaluate the same beams. LTB beam program calculates the elastic critical moment using an iterative procedure. The contrast between the theoretical and LTB beam findings and the numerical model results is summarized in Table 2. The crucial moment estimated by the numerical model agrees well with the corresponding data.

As illustrated in Figure 3, (Nsier et al. 2012) carried out three full-scale experiments on simply supported cellular beams with varying profiles under two vertical loads. The current finite element model was calibrated using the beam with section profile IPE 330. According to Fig. 3, the beam contained 17 cells, each with a diameter of 345 mm and a separation of $a = 395$ mm. There was a two-point loading scheme applied to the beam. Four 20 mm-thick stiffeners are employed at the load application and support points. At the location of the load application, the top and bottom flanges are additionally laterally braced. The yield stress and Young's modulus of the tested steel beam are 373 MPa and 173.4 GPa, respectively, based on coupon tests. The reported

experimental load of 176.9 kN and the anticipated numerical maximum load of 168.8 kN accord quite well. The mid-span deflection at failure, which is estimated at 69.8 mm, agrees well with the experimental value of 62.3 mm.

Table 2

Buckling load data from previous studies, the LTBeam software, and the numerical model

Beam length (mm)	Critical buckling moment (kN.m)		
	Kitiporanchi and Wang [5]	LTBeam program results	Numerical model results
3000	170.5	168.81	166.95
6000	54.1	53.23	52.9
9000	31.9	29.46	29.56
12000	21.81	20.03	22.91

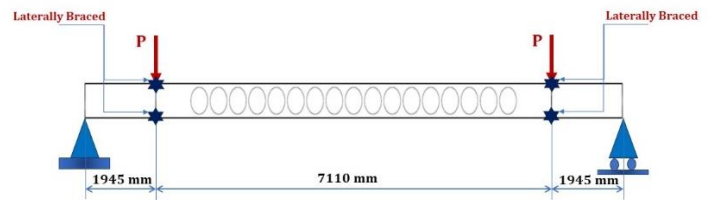


Fig. 3. Tested beam dimensions [9]

5. Results and discussion

We conducted a thorough numerical parametric analysis using the validated finite element model to assess the buckling behavior of various dimensions and configurations of T-shaped steel beams, as outlined in Table 2. For each scenario, we determined the maximum moment at buckling (M_{F-P} and M_{F-W}) induced by a mid-span concentrated load and uniform load, respectively. These values were then utilized to derive the moment gradient factor, C_b , by normalizing them against the critical moment resulting from a uniformly distributed moment load, M_{F-M} . Consequently, the moment gradient factor is defined by Equations (1) and (2) for the concentrated load and uniformly distributed load cases, respectively:

$$C_b = M_{(F-P)} / M_{(F-M)} \quad (1)$$

$$C_b = M_{(F-W)} / M_{(F-M)} \quad (2)$$

The moment gradient factor C_b variation for a series of T-shaped beams with varying spans loaded with a mid-span concentrated load and flange thicknesses of 12 mm and 6 mm, respectively, is shown in Figures. 4 and 6. The study of the beams considered three distinct stem thicknesses: 10 mm, 8 mm, and 6 mm. Additionally, consideration was given to the size of hole-to-stem ratios of 0.5, 0.6, and 0.8. Figures 4 and 6 show what is discovered to be the following:

- Since longer beams suffer the LTB mode of failure, there are no appreciable variations in the C_b value compared to the corresponding values of the thicker flange for beams of the long span. This suggests that the influence of flange thickness on the C_b value diminishes for longer spans where LTB becomes the predominant mode of failure. In essence, the behavior of longer beams under LTB conditions may be less sensitive to changes in flange thickness compared to shorter spans. This finding underscores the importance of considering span length alongside other structural parameters when assessing the susceptibility of beams to LTB failure
- In contrast to beams with a 12mm flange thickness, shorter-span beams with a 6mm flange thickness exhibit lower C_b values. The shorter beams' web distortion is responsible for this decrease. This decrease in C_b values can be attributed to the increased influence of web distortion in shorter beams with thinner flanges. The reduced flange thickness may lead to greater susceptibility to web distortion, which in turn affects the overall stability of the beam and results in lower C_b values. Therefore, the interaction between flange thickness and web distortion plays a significant role in determining the C_b values of shorter-span beams.
- Conversely, C_b values for small-length beams are less than 1.0, indicating a low likelihood of LTB and other mode failure control. This implies that the beams are effectively resistant to LTB failure, as well as other failure modes that C_b accounts for.
- T-beams exposed to an evenly distributed load exhibit similar tendencies, as illustrated in Figs. 5 and 7 for beams with flange thicknesses of 12 mm and 6 mm, respectively. The similarity in tendencies across different flange thicknesses suggests that the distribution of the load has a significant influence on the structural response of the beams, irrespective of their flange thickness. This indicates that the load distribution pattern plays a critical role in determining the overall behavior and performance of T-beams under applied loads.

Figures 5 and 7 illustrate the changes in the moment gradient factor (C_b) for a series of T-shaped beams with different spans, subjected to a uniformly distributed load, and with flange thicknesses of 12 mm and 6 mm, respectively. The analysis considered varying stem thicknesses of 10 mm, 8 mm, and 6 mm, while maintaining a constant flange thickness of 12 mm. The findings from this analysis are depicted in Figures 5 and 7:

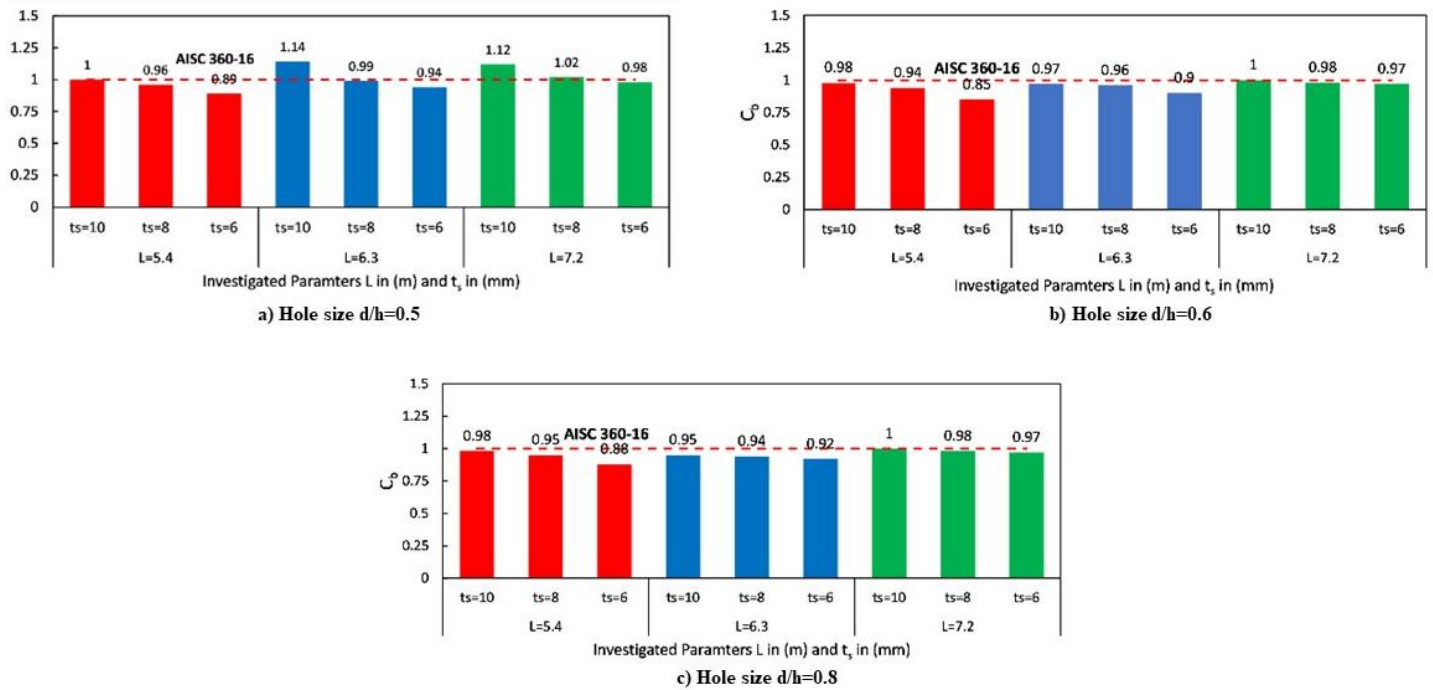


Fig. 4. Moment gradient factor for beams with ($t_f=12\text{mm}$) under concentrated mid-span load. a) Opening size ($d/h=0.5$). b) Opening size ($d/h=0.6$). c) Opening size ($d/h=0.8$).

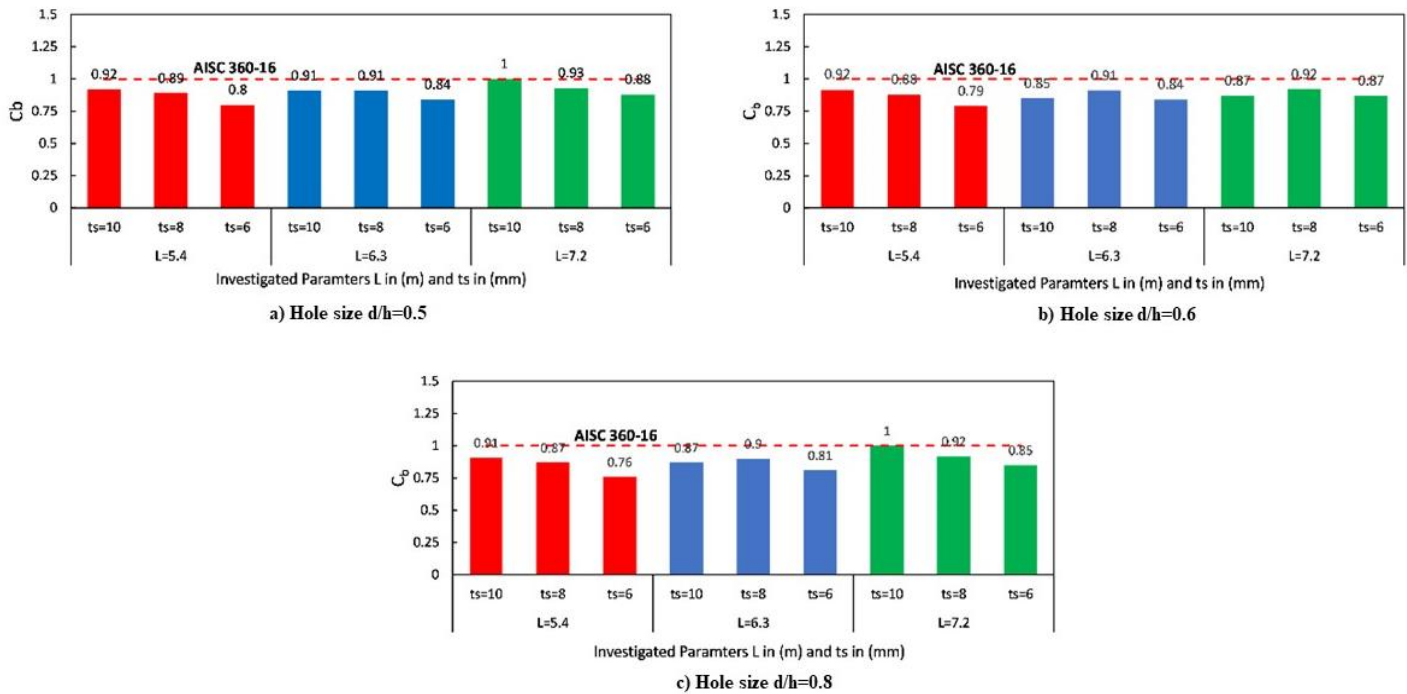


Fig. 5. Moment gradient factor for beams with ($t_f=12\text{mm}$) under uniform distributed load. a) Opening size ($d/h=0.5$). b) Opening size ($d/h=0.6$). c) Opening size ($d/h=0.8$).

- Beams subjected to mid-span concentrated load usually have lower C_b values than beams with uniformly distributed loads. This observation

suggests that concentrated loading at the mid-span induces higher levels of stress and deformation in the beams, leading to a decreased capacity to resist

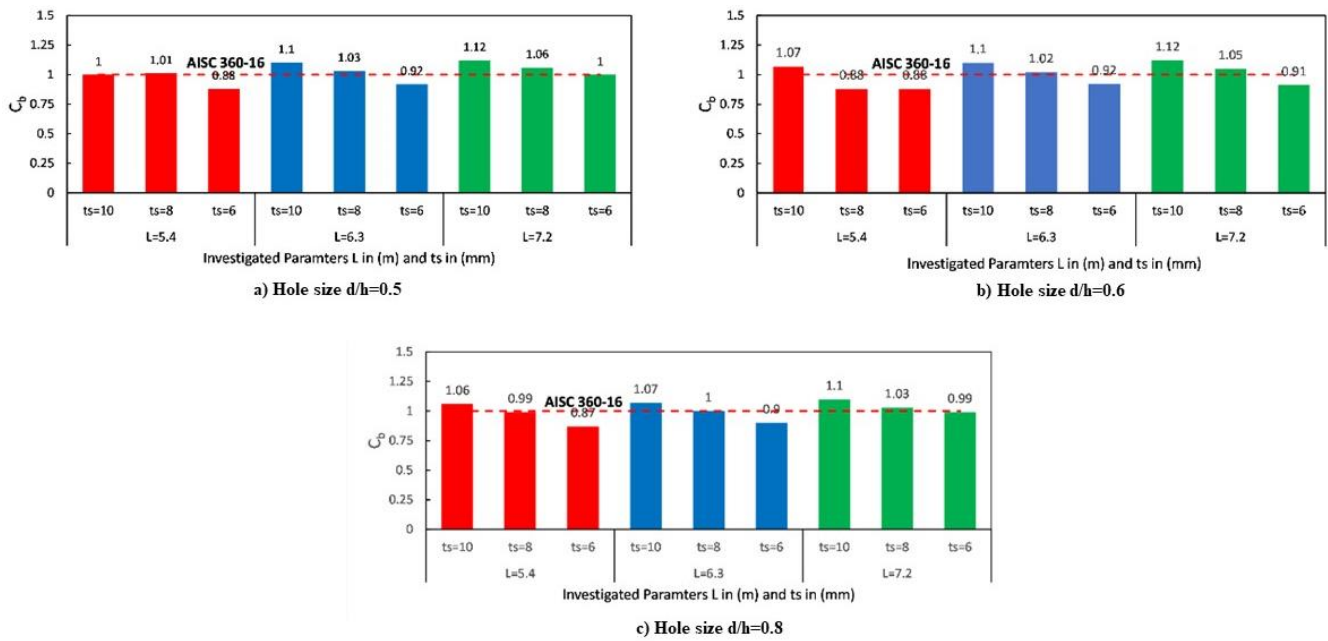


Fig. 6. Moment gradient factor for beams with ($t_f=6\text{mm}$) under concentrated mid-span load. a) Opening size ($d/h=0.5$). b) Opening size ($d/h=0.6$). c) Opening size ($d/h=0.8$).

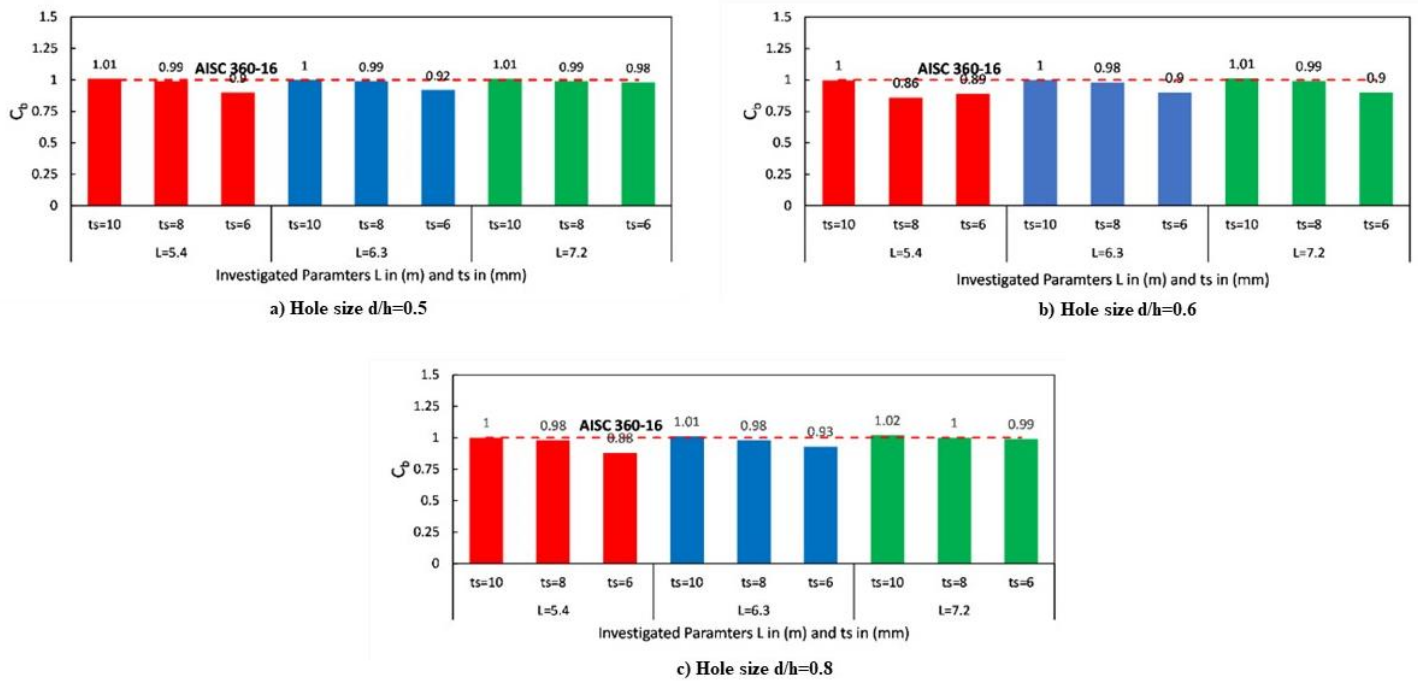


Fig. 7. Moment gradient factor for beams with ($t_f=6\text{mm}$) under uniform distributed load. a) Opening size ($d/h=0.5$). b) Opening size ($d/h=0.6$). c) Opening size ($d/h=0.8$).

lateral-torsional buckling (LTB) and other failure modes accounted for by C_b . The lower C_b values indicate a higher vulnerability to buckling and other forms of failure in beams subjected to mid-span concentrated loads, highlighting the importance of

load distribution patterns in assessing the structural stability and performance of beams.

- C_b values generally rise as beam span increases, where LTB failure mode control occurs.

- Conversely, C_b values for small-length beams are less than 1.0, indicating a low likelihood of LTB and other mode failure control.
- T-beams exposed to uniformly distributed load exhibit similar tendencies, for the examined opening widths. Under the mid-span focused load, C_b 's values are significantly lower than those of its contemporaries. This variation in C_b levels is explained by the widespread compression across a longer range of time, which lowers the C_b value.

6. Conclusion and Recommendations

We investigate lateral-torsional buckling in T-shaped beams with apertures using a three-dimensional finite element model with linear and nonlinear material models. The modeling parameters provide a strong basis for our work, having been rigorously tested against theoretical, numerical, and experimental results from the literature. Using a detailed parametric numerical analysis, we examine the effects of several stem opening configurations (d/h at 0.5, 0.6, and 0.8) and flange thickness values (12mm, 6mm) as well as varied stem thicknesses (10mm, 8mm, and 6mm). The purpose of this analysis is to assess how stem opening widths, flange, stem dimensions, and other factors affect lateral-torsional buckling in T-shaped beams with openings.

Our conclusions provide important insights into the lateral-torsional buckling behavior of T-shaped beams by summarizing the findings within the investigated model and parameter range:

- Long-span beams are found to have a larger LTB moment than short-span beams, particularly when lateral-torsional buckling is used to regulate the failure mode.
- Short-span beams exhibit web distortion, which lowers the values of the LTB moments.
- The precise calculation of the C_b value of 1.0, as denoted by various codes, is necessary for T-shaped beams with stem apertures and thinner stems.
- The LTB moment is stronger in T-shaped beams with significant flange thickness, which highlights the subsequent influence of stem apertures.

There are further studies which may be done in this field such as take the effect of temperature on T-section with opening instead of distribution and concentrated load and may be investigated in different conditions in future studies.

7. Reference

- [1] M. G. Salvadori, Lateral buckling of I-beams, Transactions of the American Society of Civil Engineers 120 (1) (1955) 1165-1177.
- [2] S. P. Timoshenko and J. M. Gere, Theory of Elastic Stability, Theory of Elastic Stability, 2 (1961).
- [3] D. A. Nethercot, A unified approach to the elastic lateral buckling of beams, The structural engineer 49(7) (1971).
- [4] E. Wong, and R. G. Driver, Critical evaluation of equivalent moment factor procedures for laterally unsupported beams, Engineering Journal 47(1) (2010).
- [5] S. Kitipornchai, and C. M. Wang, Lateral buckling of tee beams under moment gradient, Computers & structures 23(1) (1986) 69-76.
- [6] M. Manarin, R. G. Driver, and Y. Li, Moment Gradient Factor for Lateral-Torsional Buckling of T-shaped Beams, Proceedings of the Annual Stability Conference, Structural Stability Research Council, Louis, Missouri April, 2019, pp. 2-54.
- [7] R. Gonçalves, and D. Camotim, Geometrically nonlinear generalized beam theory for elastoplastic thin-walled metal members, Thin-walled structures 51 (2012) 121-129.
- [8] B. Kim, L. Y. Li, and A. Edmonds, Analytical solutions of lateral-torsional buckling of castellated beams, International Journal of Structural Stability and Dynamics, 16(08) (2016).
- [9] R. M. Lawson, Design for openings in the webs of composite beams, CIRIA Special Publication and SCI Publication 068. (1987).
- [10] D. Darwin, Steel and composite beams with web openings, Steel Design Guide Series No. 2. Chicago: American Institute of Steel Construction (1990).
- [11] P. R. Knowles, Castellated beams. Proceeding of the Institution of Civil Engineers, ICE, London, U.K. 1991.
- [12] R. G. Redwood, Cho SH. Design of steel and composite beams with web openings, J Constr Steel Res 25 (1993) 23-41.
- [13] R. A. Bhat, and L. M. Gupta, Moment-gradient factor for perforated cellular steel beams under lateral torsional buckling, Arabian Journal for Science and Engineering, 45(10) (2020) 8727-8743.
- [14] D. Sonck, and J. Belis, Lateral-torsional buckling resistance of cellular beams, Journal of Constructional Steel Research 105 (2015) 119-128.
- [15] P. Panedpojaman, W. Sae-Long, and T. Chub-uppakarn, Cellular beam design for resistance to inelastic lateral-torsional buckling, Thin-Walled Structures 99 (2016) 182-194.
- [16] L. Subramanian, and D. W. White, Reassessment of the lateral torsional buckling resistance of I-section members: uniform-moment studies, Journal of Structural Engineering 143(3) (2017)
- [17] F. P. V. Ferreira, A. Rossi, and C. H. Martins, Lateral-torsional buckling of cellular beams according to the possible updating of EC3. Journal of Constructional Steel Research

153 (2019) 222-242.

- [18] K. M. El-Sawy, A. M. Sweedan, and M. I. Martini, Moment gradient factor of cellular steel beams under inelastic flexure, *Journal of Constructional Steel Research* 98 (2014) 20-34.
- [19] A. M. Sweedan, Elastic lateral stability of I-shaped cellular steel beams, *Journal of Constructional Steel Research*, 67(2) (2011) 151-163.
- [20] Ellobody, E. Nonlinear analysis of cellular steel beams under combined buckling modes. *Thin-walled structures*, 2012, 52, 66-79.
- [21] E. Ellobody, Nonlinear analysis of cellular steel beams under combined buckling modes, *Thin-walled structures* 52 (2012) 66-79.
- [22] ABAQUS 6.12 [Computer software]. Dassault Systèmes, Waltham, MA.
- [23] ECP-205 (ASD), Egyptian Code of Practice for Steel Construction and Bridges. Housing and Building Research Center, 2011.
- [24] ECP-205 (LRFD), Egyptian Code of Practice for Steel Construction and Bridges. Housing and Building Research Center, 2011.
- [25] AISC. Specification for Structural Steel Buildings, ANSI / AISC 360-16. AISC, Chicago, 2016.